

Archived in

dspace@nitr

<http://dspace.nitrkl.ac.in/dspace>

S S Panda is presently with National Institute of Technology Rourkela

sspanda@nitrkl.ac.in

Published in

Journal of Materials Processing Technology

Volume 172, Issue 2, 28 February 2006, Pages 283-290

<http://dx.doi.org/10.1016/j.jmatprotec.2005.10.021>

Drill Wear Monitoring using Back Propagation Neural Network

S. S. Panda, A.K Singh, D. Chakraborty*,

Mechanical Engineering Department

Indian Institute of Technology Guwahati, Guwahati 781 039, India

and

S. K. Pal

Mechanical Engineering Department

Indian Institute of Technology Kharagpur, Kharagpur 721 302, India

Abstract

Present work deals with prediction of flank wear of drill bit using back propagation neural network (BPNN). Drilling operations have been performed in mild steel work-piece by high-speed steel (HSS) drill bits over a wide range of cutting conditions. Important process parameters have been used as input for BPNN and drill wear has been used as output of the network. Inclusion of chip thickness as an input in addition to conventional parameters leads to better training of the network. Performance of the neural network has been found to be satisfactory while validated with experimental result.

Keywords: Flank wear; Artificial neural network; Drilling; Chip thickness.

1. Introduction

Drill wear is a very important issue in manufacturing industries. Drill wear not only affects the surface roughness of the hole, but also influences the life of the drill bit.

Wear in drill bit is characterized as flank wear, chisel wear, corner wear and crater wear. Since wear on drill bit dictates the hole quality and tool life of the drill bit, online monitoring and prediction of drill wear is an important area of research. Many works have been reported in the broad field of tool condition monitoring.

Lin and Ting [1] studied the effect of tool wear as well as other cutting parameters on the current force signals, and established the relationship between the force signals and tool wear as well as the other cutting parameters.

* Corresponding author. Tel: +91-361-2582666; fax: +91-361-2690762.

E-mail address: chakra@iitg.ernet.in (D. Chakraborty).

Lin and Ting [2] in another work used back propagation neural network with sample and batch mode, and observed faster convergence of error in the case of sample mode. EI-Wardany *et al.* [3] used the vibration signal in drill condition monitoring. They presented a study using the kurtosis of the time domain and area under the power spectrum curve to monitor various type of drill wear. Lee *et al.* [4] used the abductive network modeling for drilling process for predicting the tool life, tool wear and surface roughness. Optimal network architecture is prepared based on predicted square error criterion. Li and Tso [5] used the regression model for monitoring the tool wear based on current signals of spindle motor and feed motor. Liu *et al.* [6] used the algorithm for synthesis of polynomial network for predicting (ASPNS) the corner wear in drilling operation. Choudhury and Raju [7] developed a regression model to measure the flank wear and corner wear of a drill bit in cutting operation. Kim *et al.* [8] used the william drill model for predicting and validating the progressive drill wear based on spindle motor power consumption. Davim and Antonio [9] used the evolution strategy for identifying the type of wear in polycrystalline diamond (PCD) drill bit with metal matrix composite as work-piece. They used the pareto optimal solution in the genetic algorithm for maximization of tool life and minimization of drill wear. Ertunc and Loparo [10] used decisions fusion center algorithm (DFCA) for monitoring online tool wear condition in drilling process, and used various numerical methods for predicting the condition of tool wear land. Tsao [11] used the radial basis function network (RBFN), and adaptive based radial basis

function network (ARBFN) to predict the flank wear, and compared their result with experimentally obtained data. Nouari *et al.* [12] used the third wave advantage software for predicting the tool chip interface temperature, which is major factor for drill wear formation in the dry condition. Abbu [13] used the vibration signature analysis for predicting the wear rate in drilling. He estimated three different patterns of vibration signature like harmonic wavelets coefficient, power spectra density and first fourier transformation (FFT). All these are inputs to the neural network model. Kim and Ramulu [14] used multiple objective linear programming models for optimizing drill hole quality with different cutting conditions such as speed and feed-rate.

2. Back propagation neural network

Back propagation neural network (BPNN) has been used in the present work. Basic structure of back propagation neural network having input, hidden and output layers, is shown in Fig. 1. Input layer receives information from the external sources, and passes this information to the network for processing. Hidden layer receives information from the input layer, and does all the information processing, and output layer receives processed information from the network, and sends the results out to an external receptor. The input signals are modified by interconnection weight, known as weight factor w_{ij} , which represents the interconnection of i^{th} node of the first layer to j^{th} node of the second layer. The sum of modified signals (total activation) is then modified by a *sigmoidal* transfer function.

Batch mode type of supervised learning has been used in the present case, where, all input-output pattern sets are presented to the neural network one by one, and then adjusted using average gradient information. During training, the calculated output is compared with the target output, and the mean square error is calculated. If the mean square error is more than a prescribed limiting value error, it is back propagated *i.e.*, from output to input then weights are further modified till the error is within a prescribed limit.

Mean square error E , is calculated by the equation (1),

$$E = \frac{1}{2} \left(\sum_{p=1}^p \sum_{k=1}^n (d_k^p - c_k^p)^2 \right) \quad (1)$$

where,

p = Number of pattern

n = Number of node in output layer

d_k^p = Desired output of k^{th} node of p^{th} pattern

c_k^p = Calculated out put of k^{th} node of p^{th} pattern

3. Experimental set-up

Large number of experiments over a wide range of cutting conditions has been performed. In the present work, flank wear has been considered. Fig. 2 shows a schematic representation of the experimental set up used in present work.

Radial drilling machine (Batliboi Limited, BR618 model) is used for the drilling operation. HSS drill bits with different diameters have been used for drilling in mild steel work-piece at different cutting conditions. Thrust force and torque are recorded through a piezo-electric Kistler 9272 dynamometer. Signal from the dynamometer is amplified through charge amplifier, and is stored in the computer through data acquisition system. Charge amplifiers of B&K 2525 model and Advantech PCL 818 HG model data acquisition system are used in present work. Thickness of chip for each cutting condition is measured using micrometer. Flank wear is measured by the digital microscope with the help of Karl-Zeiss software interfacing. The maximum flank wear is used as the criterion to characterize the drill condition, and is obtained by measuring the wear at different points on either of the cutting edge. Photographs of gradual wear build-up process for three different feed-rates are shown in Fig. 3(a)-3(c).

4. Results and discussion

Drilling operation has been conducted over a wide a range of cutting condition. Spindle speed has been varied in the range 315 rpm to 1000 rpm in six steps. Feed-rate has been varied from 0.13 to 0.71 mm/rev in six steps. HSS drill bit of three different diameters have been used for drilling holes in mild steel plates. Various combination of spindle speed, feed-rate and drill diameter has been used to perform 52 different drilling operations. For each of these conditions, thrust force and torque have been measured using the dynamometer, and the data is stored in the computer through the data acquisition system. Also corresponding to each cutting condition, maximum flank wear has been measured using digital microscope with interface of Karl-Zeiss software. For each cutting condition, the average thickness of chip is measured using the micrometer. The results of the experiment are tabulated in Table 1.

4.1. Effect of important parameters on thrust force and torque

Figs. 4-10 show the effect of important cutting parameters on thrust force and torque during drilling operation. From Figs. 4-5 and Figs. 7-8 it could be observed that thrust force and torque increase as drill diameter and feed rate increase. This is due to increase of the un-deformed chip thickness, which is known as size effect [2]. It has also been observed that drill diameter has more effect on thrust force and torque than that of feed-rate, and as a result both thrust force and torque increase sharply beyond 7.5 mm drill diameter. It may be due to increase of thickness of un-deformed chip with increase of drill diameter than that of feed rate. Increase of drill diameter along the circumferential direction imparts more chip load than that of increase in feed rate along the axial direction. Fig. 6 and Fig. 9 show that thrust force and torque decrease with increasing spindle speed. This is due to high temperature generation at the tool chip interface, and thus the strength of the work material reduces [2].

4.2. Wear prediction by neural network

Back propagation neural network algorithm has been used in the present work. To train the neural network thrust force, torque, chip thickness, spindle speed, feed-rate and drill diameter are used as input parameters and corresponding maximum flank

wear has been used as the output parameter as shown in Fig. 1. From the 52 data sets obtained from the experiment, 39 have been selected at random for training the network, and remaining 13 are used for testing. The normalized data sets are used for training the network. The data sets are normalized in the range of 0.1 to 0.9 by using equation (2).

$$y = 1 + 0.8 \left(\frac{x - x_{\min}}{x_{\max} - x_{\min}} \right) \quad (2)$$

where,

x = Actual value,

x_{\max} = Maximum value of x ,

x_{\min} = Minimum value of x ,

y = Normalized value corresponding to x .

The number of hidden layer, number of nodes in the hidden layer, learning rate (η), and momentum coefficient (α) are decided by trial and error.

4.2.1. *Neural network architecture without chip thickness*

Different combination of learning rate (η), and momentum coefficient (α) and number of hidden layer have been tried. Depending upon the mean square error and convergence rate, optimum network architecture has been arrived at. In the present case, 5-4-1 network with $\eta = \alpha = 0.3$ has been found out to be the optimum network (Table 2). Fig. 10 shows the variation of training and testing error with number of iteration for the network used in the present case. The wear predicted by the neural network has been compared with the corresponding actual experimental values and are shown in Fig. 11. It could be observed from the figure that the predicted wear is within $\pm 7.5\%$ of the actual experimental values of the flank wear.

4.2.2. *Neural network architecture with chip thickness*

An attempt has been made to study the effect of including chip thickness as an input to the neural network in addition to the input used in the earlier network (5-3-1).

Best network architecture has been again arrived at by trial and error of different combination of learning rate (η), momentum factor (α) and number of hidden nodes. Table 3 shows some of the combinations tried and corresponding mean square error and number of iterations. Depending upon the mean square error and the convergence rate, 6-5-1 network with $\eta=0.8$ and $\alpha=0.7$ has been found to be optimum network in the present case. Fig. 12 shows the variation of mean square error for the 6-5-1 network with $\eta=0.8$ and $\alpha=0.7$. It could be observed that mean square error value is not only much lower compared to the 5-3-1 network used earlier but also arrived at much less number of iteration. Predicted values of flank wear have been compared with corresponding actual measured values and shown in Fig. 13. It could be observed that the predicted values are within $\pm 2.5\%$ of the actual values which is much less compared to the network used earlier 5-3-1(without chip thickness).

5. Conclusions

A methodology for prediction of drill wear using back propagation neural network has been developed. Effect of various important parameters on thrust force and torque has been studied. Present study shows that back propagation neural network could be trained for future prediction of flank wear during drilling operation. It has also been observed that inclusion of chip thickness as input to the neural network not only reduces mean square training error but also it is achieved at a much less number of iteration. The predicted wear from neural network is very close to the actual wear measured experimentally.

References

- [1] S.C. Lin, C.J. Ting, Tool wear monitoring in drilling using force signals, *International Journal of Machine Tools and Manufacture*. 180 (1995): 53-60.
- [2] S.C. Lin, C.J. Ting, Drill wear monitoring using neural network, *International Journal of Machine Tools and Manufacture*. 36 (1996): 465-475.

- [3] T.I. El-Wardany, D. Goa, M.A. Elbestawi, Tool condition monitoring in drilling using vibration signature analysis, *International Journal of Machine Tools and Manufacture*. 36(6) (1996): 687-711.
- [4] B.Y. Lee, H.S. Liu, Y.S. Tarn, Modeling and optimization of drilling process. *Journal of Material Processing Technology*. 74 (1998): 149-157.
- [5] L. Xiaoli, S.K. Tso, Drill wear monitoring based on current signals, *Wear*. 231 (1999): 172-178.
- [6] H.S. Liu, B.Y. Lee, Y.S. Tarn, In-process prediction of corner wear in drilling operations, *Journal of Material Processing Technology*. 101 (2000): 152-158.
- [7] S.K. Choudhury, G. Raju, Investigation into crater wear in drilling, *International Journal of Machine Tools and Manufacture*. 40 (2000): 887-898.
- [8] H.Y. Kim, J.H. Ahn, S.H. Kim, S. Takata, Real-time drill wear estimation based on spindle motor power, *Journal of Material Processing Technology*. 124 (2000): 267-273.
- [9] J.P. Davim, C.A.C. Antonio, Optimal drilling particulate metal matrix composites based on experimental and numerical procedures, *International Journal of Machine Tools and Manufacture*. 41 (2001):21-31.
- [10] H.M. Ertunc, K.A. Loparo, A decision fusion algorithm for tool wear condition monitoring in drilling, *International Journal of Machine Tools Manufacture*. 41 (2001): 1347-1362.
- [11] C.C. Tsao, Prediction of flank wear of different coated drills for JIS SUS 304 stainless steel using neural network, *Journal of Material Processing Technology*. 123 (2002): 354-360.
- [12] M. Nouari, G. List, F. Girot, D. Coupard, Experimental analysis and optimization of tool wear in dry machining of aluminium alloys, *Wear*. 255 (2003): 1359-1368.
- [13] I. Abbu-Mahfouz, Drilling wear detection and classification using vibration signals and artificial neural network, *International Journal of Machine Tools Manufacture*. 43 (2003): 707-720.
- [14] D. Kim, M. Ramulu, Drilling process optimization for graphite/bismaleimide-titanium alloy stack, *Composite Structures*. 63 (2004): 101-114.

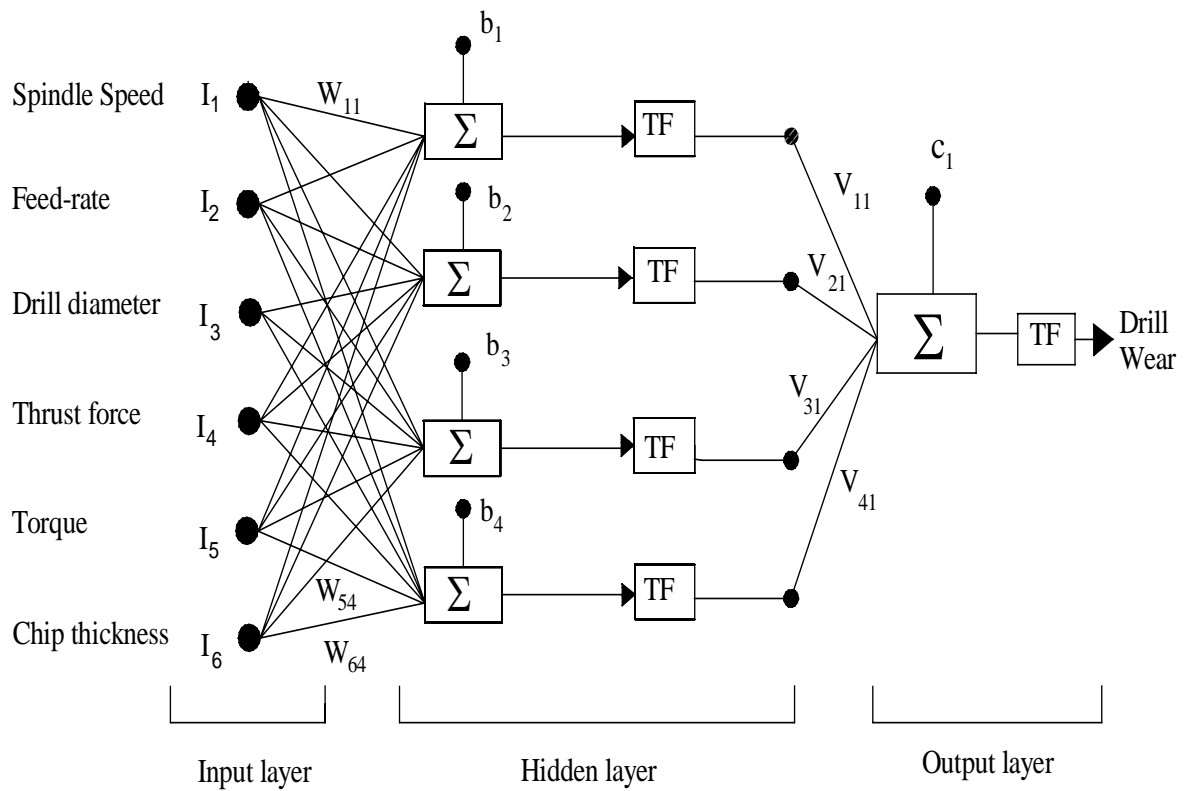


Fig. 1. Neural network with six input nodes and one output node.

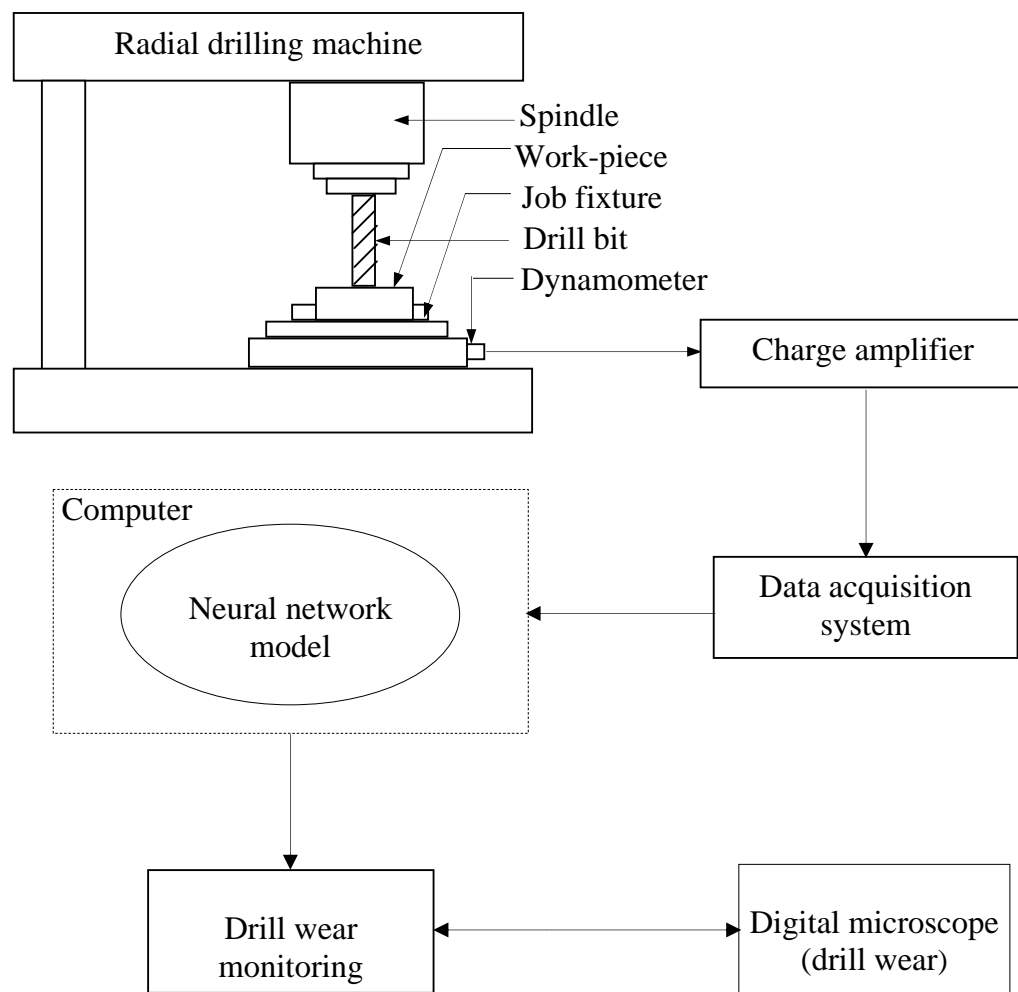


Fig. 2. Schematic diagram of the experimental set-up.

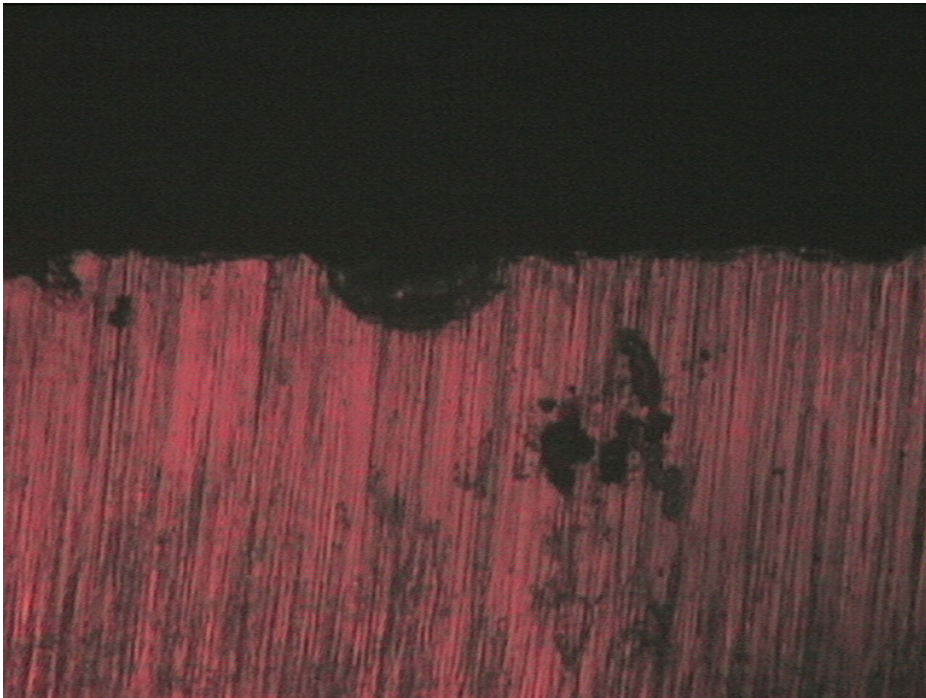


Fig. 3(a). Flank wear at diameter 10 mm, spindle speed 500 rpm, and feed-rate 0.13 mm/rev (Drill bit : HSS, Work-piece : Mild steel).

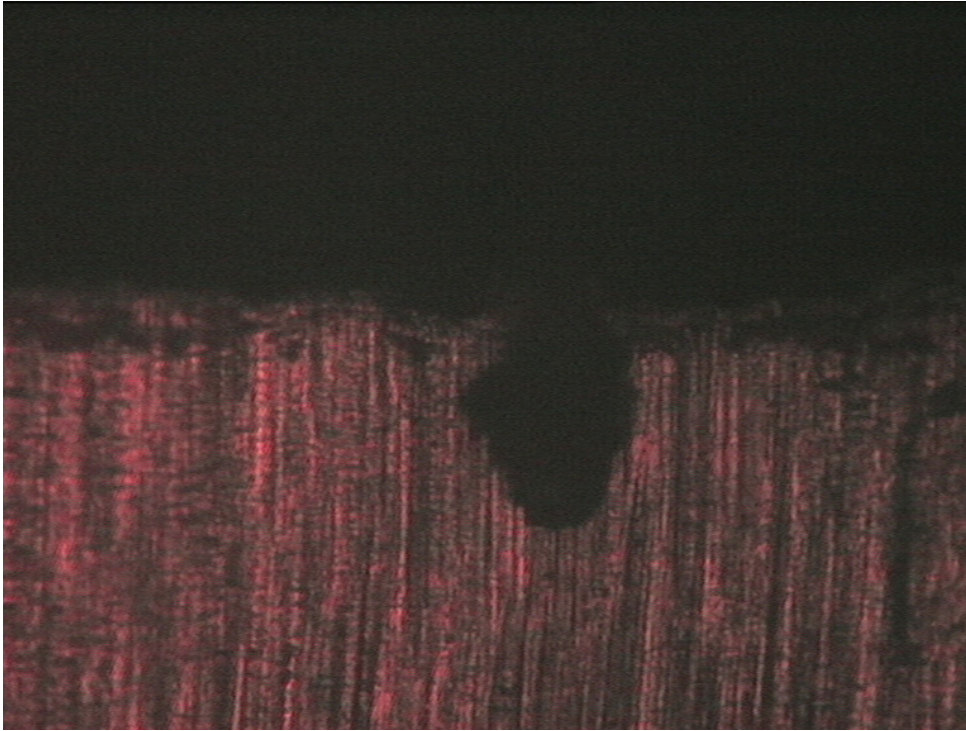


Fig. 3(b). Flank wear at diameter 10 mm, spindle speed 500 rpm, and feed-rate 0.18 mm/rev (Drill bit : HSS, Work-piece : Mild steel).

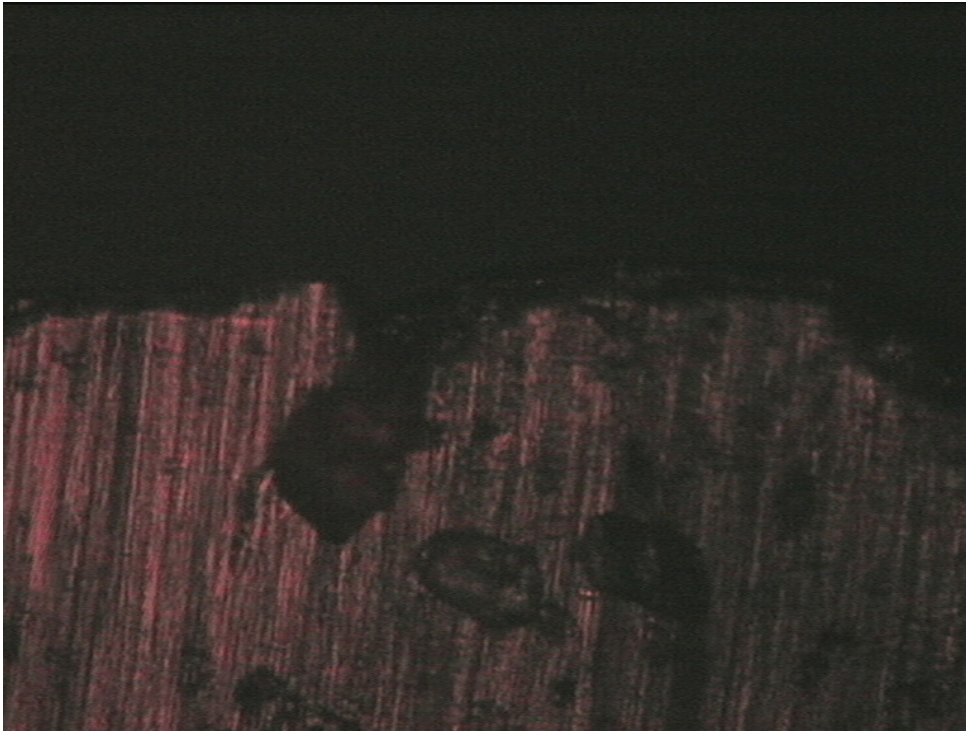


Fig. 3(c). Flank wear at diameter 10 mm, spindle speed 500 rpm, and feed-rate 0.25 mm/rev (Drill bit : HSS, Work-piece : Mild steel).

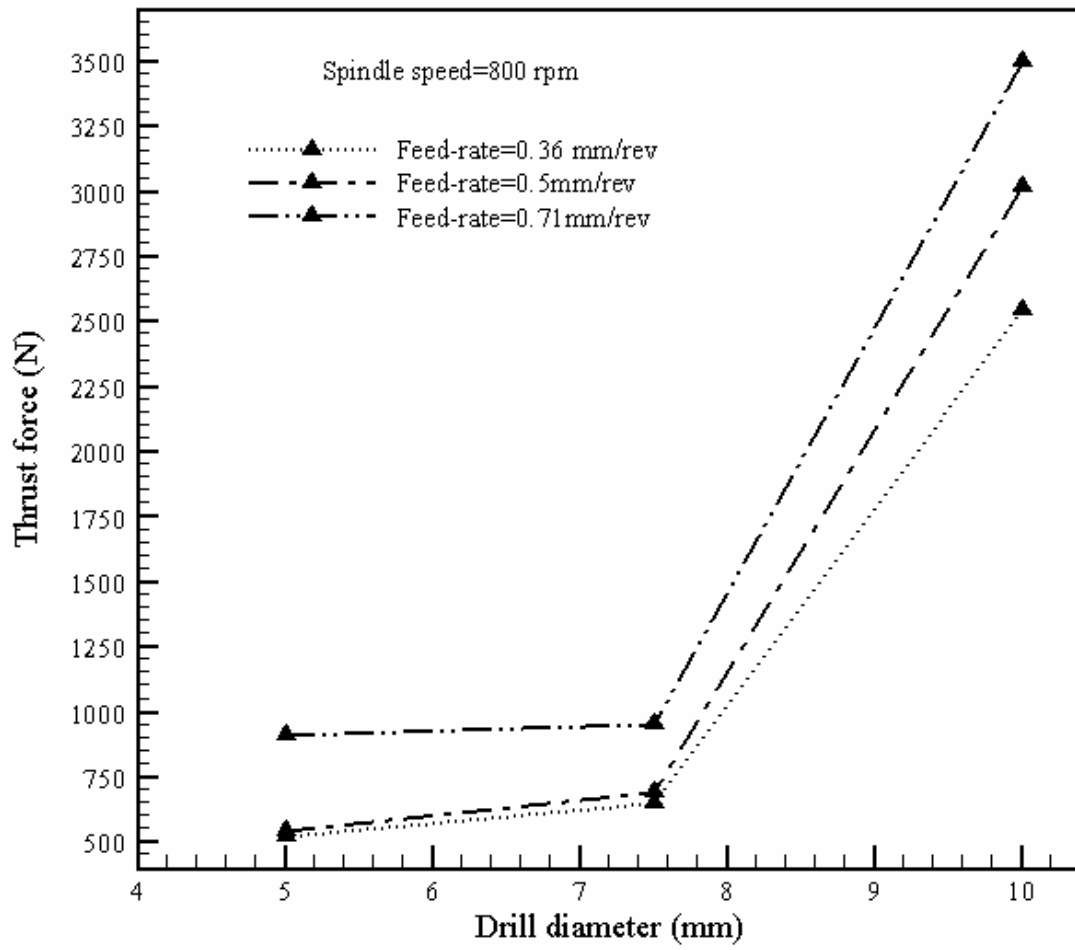


Fig. 4. Variation of average thrust force with drill diameter at different feed-rates.

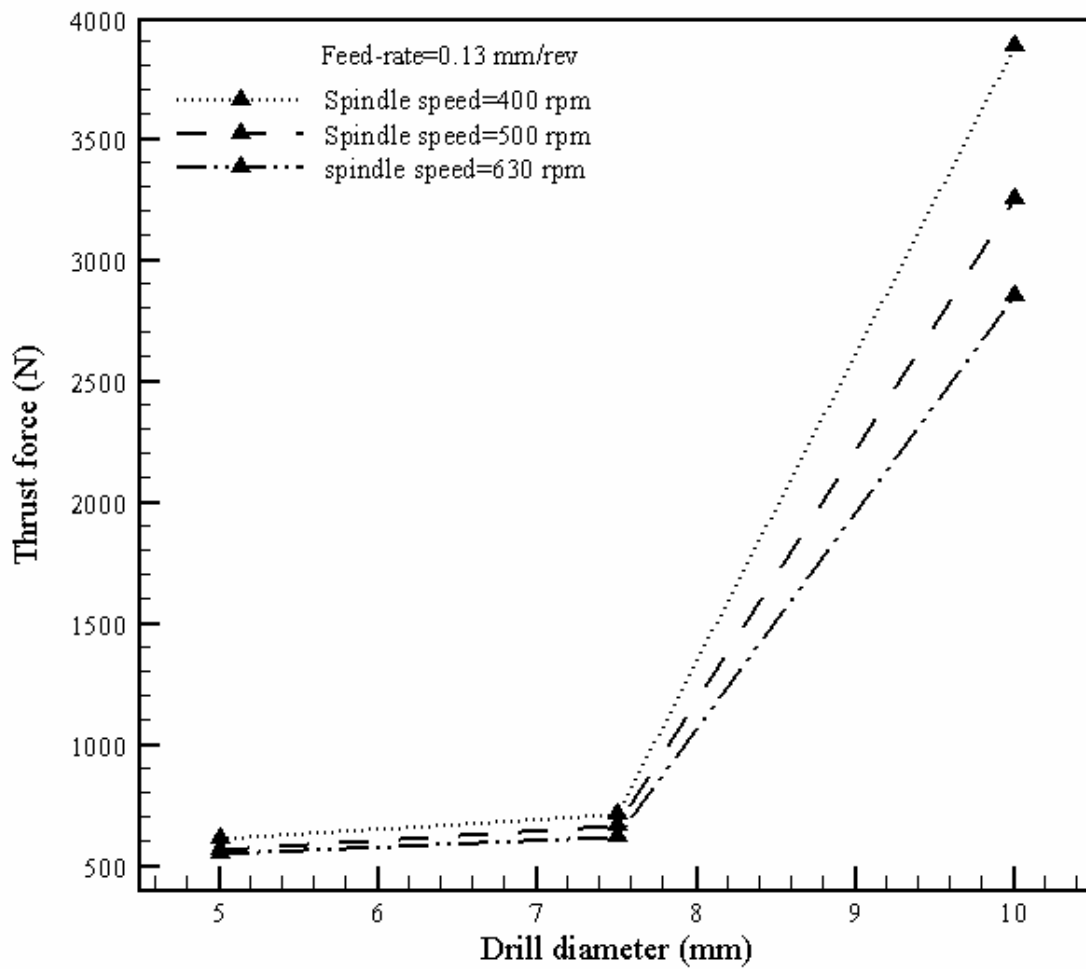


Fig. 5. Variation of average thrust force with drill diameter at different speeds.

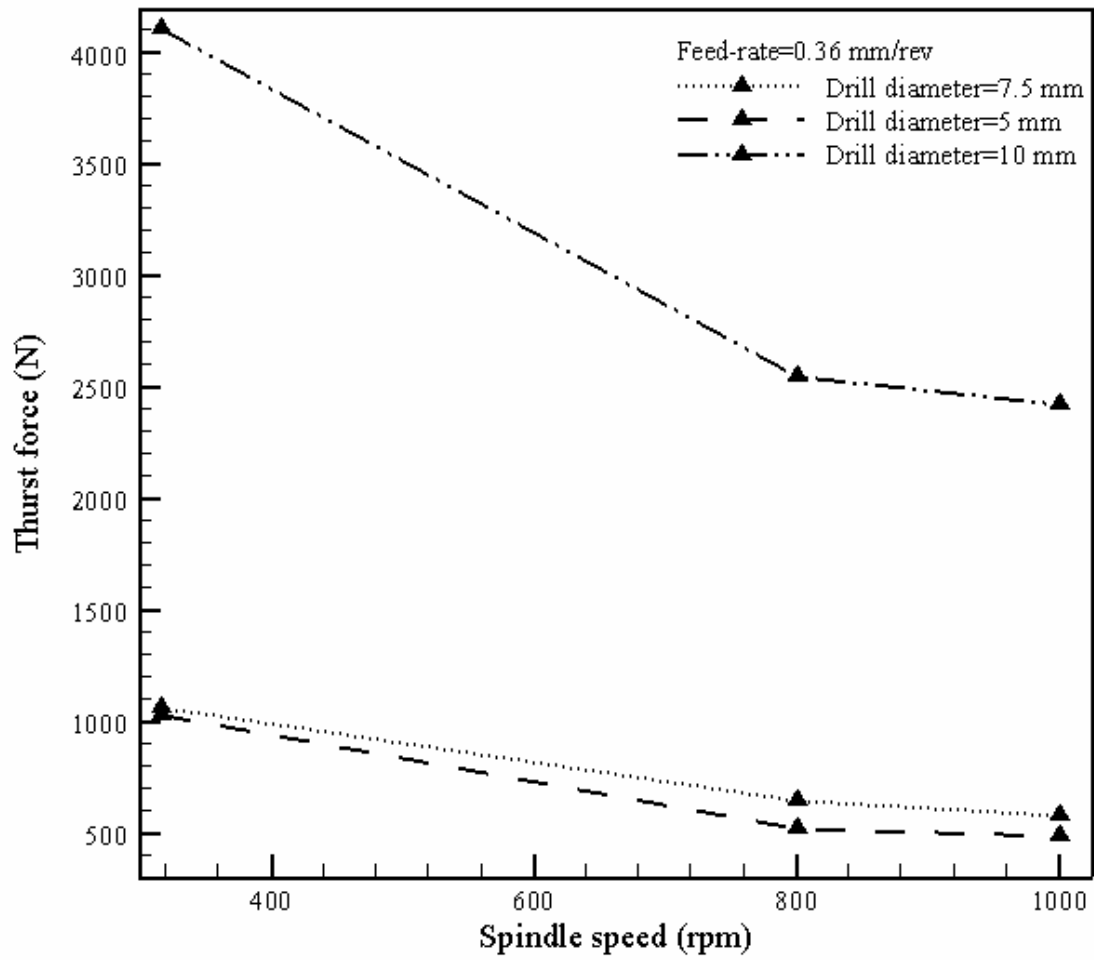


Fig. 6. Variation of average thrust force with spindle speed for different drill diameters.

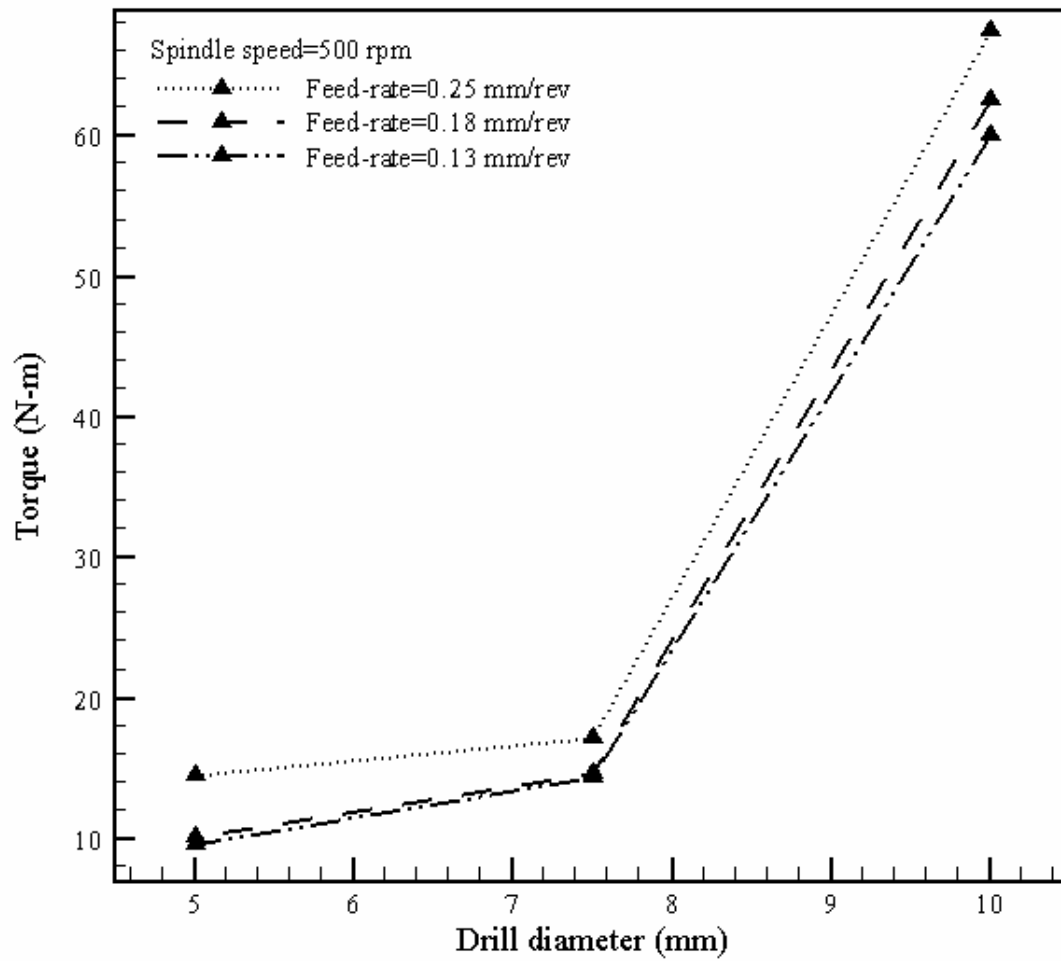


Fig. 7. Variation of average torque with drill diameter at different feed-rates.

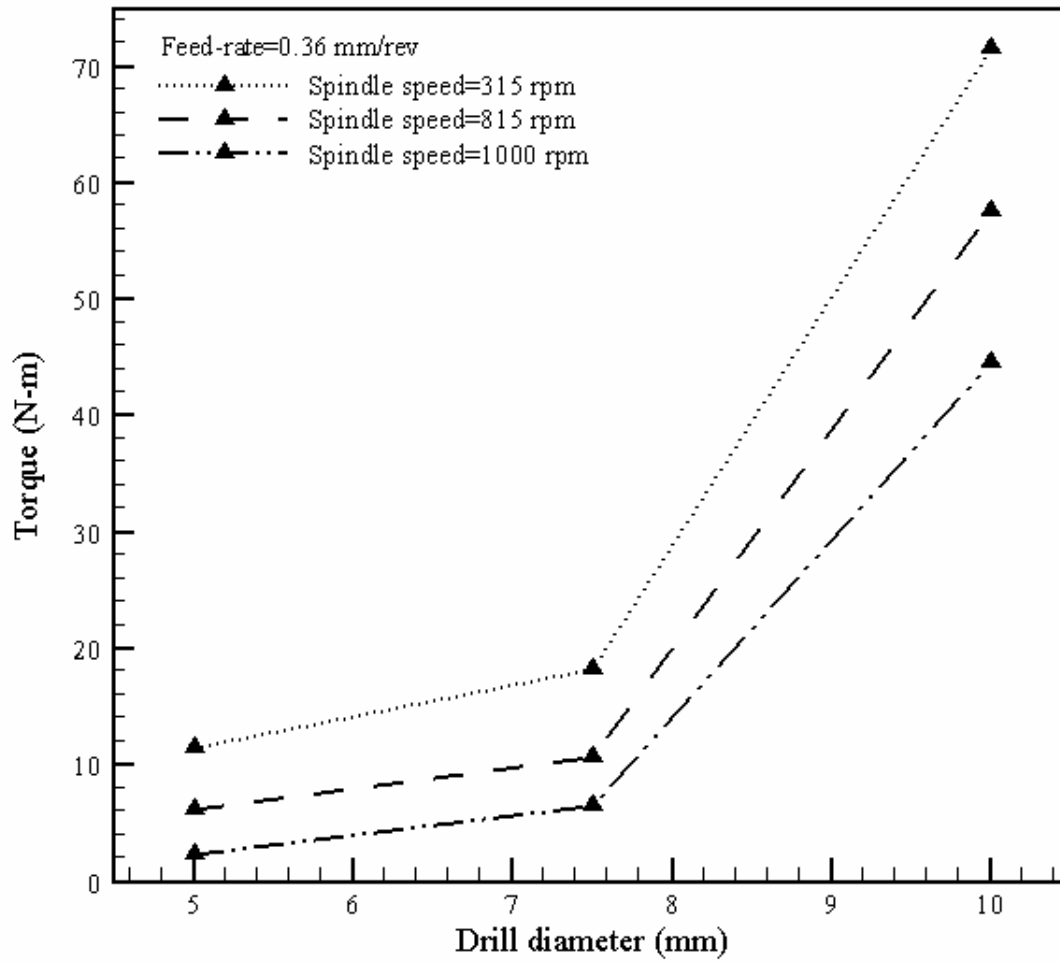


Fig. 8. Variation of average torque with drill diameter at different speeds.

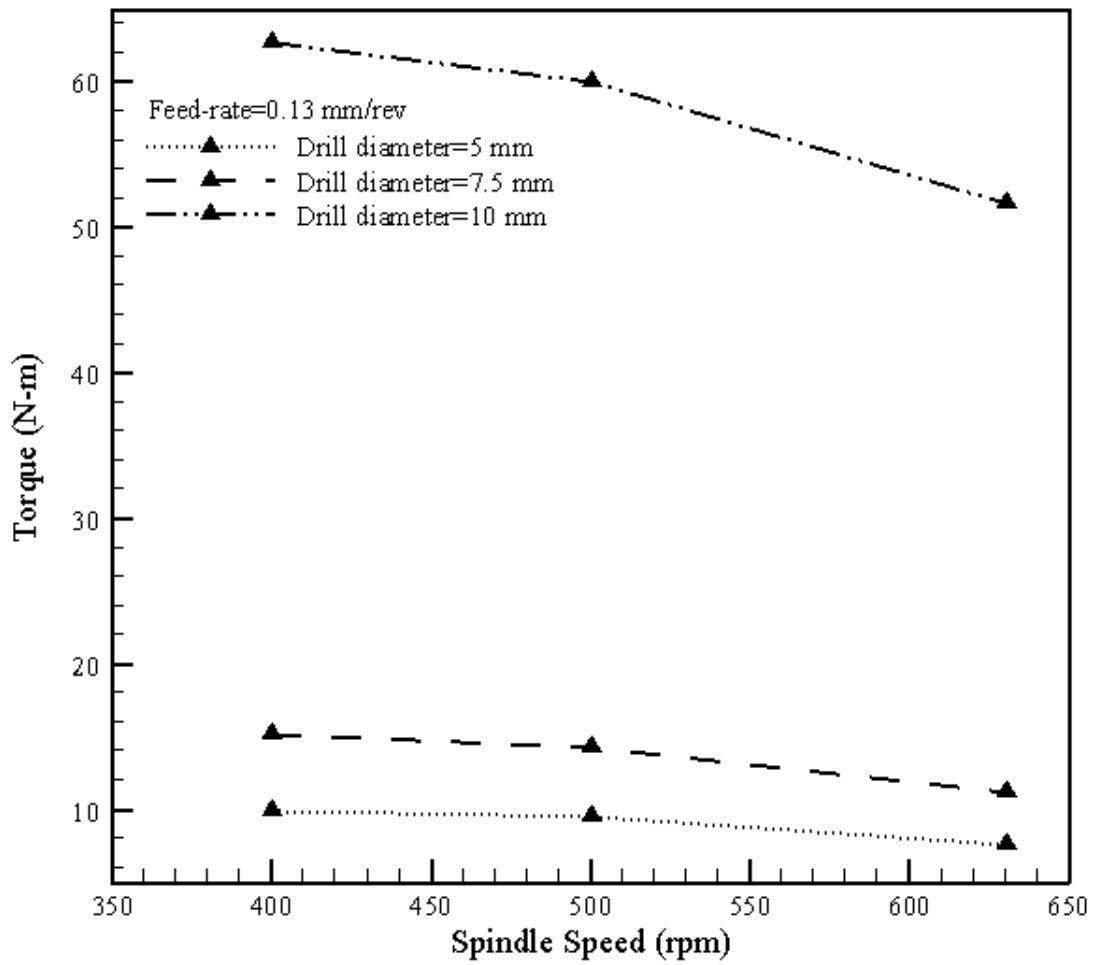


Fig. 9. Variation of average torque with spindle speed for different drill diameters.

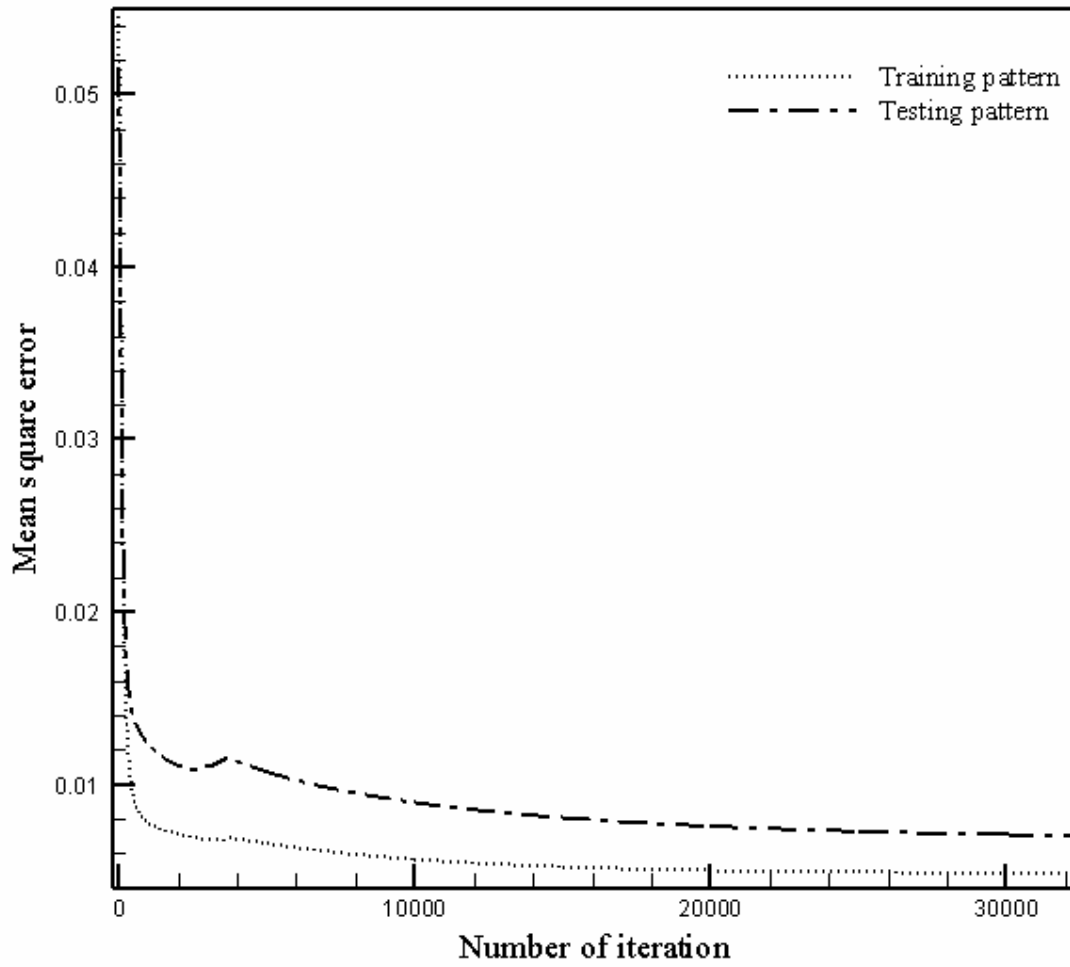


Fig. 10. Variation of mean square error with number of iteration for 5-3-1 neural network with $\alpha=0.3$, $\eta=0.3$ (without considering chip thickness).

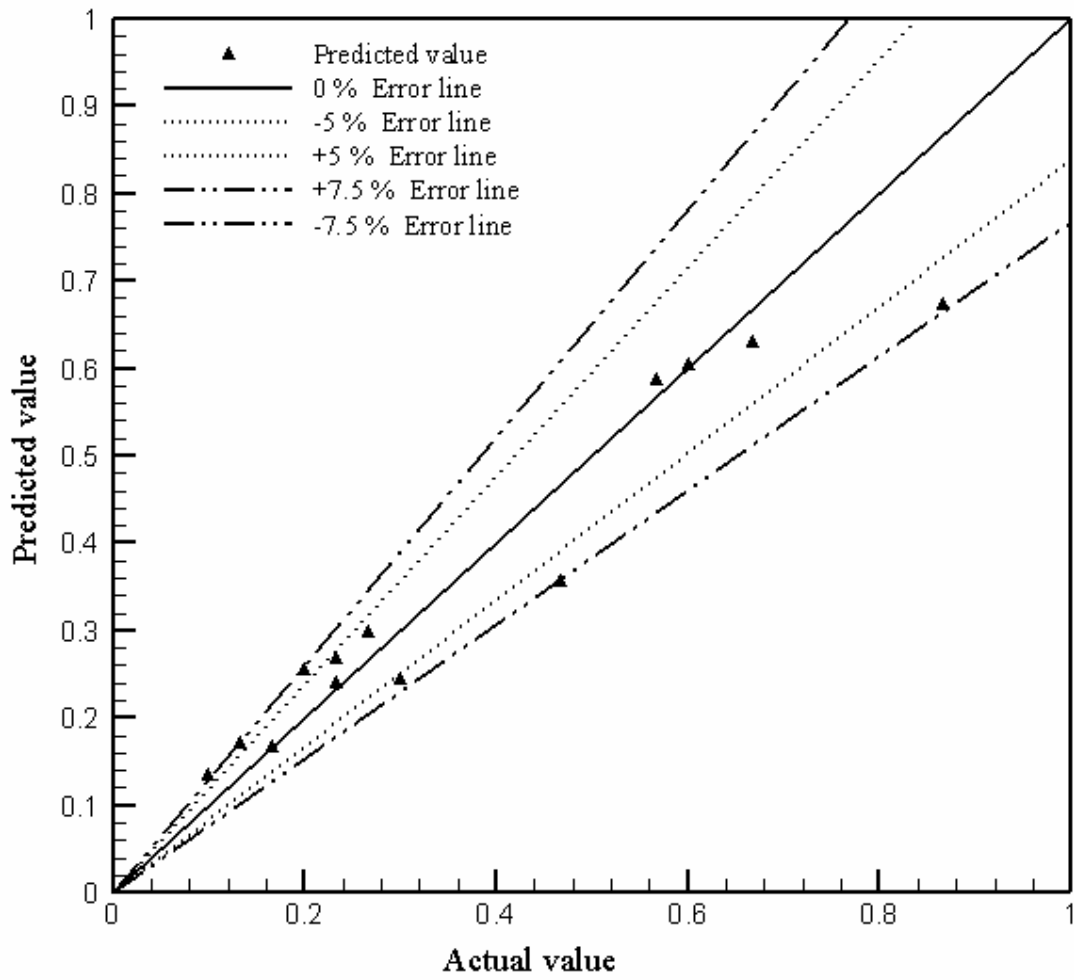


Fig. 11. Comparison between experimental value and predicted value of flank wear by 5-3-1 neural network (without considering chip thickness).

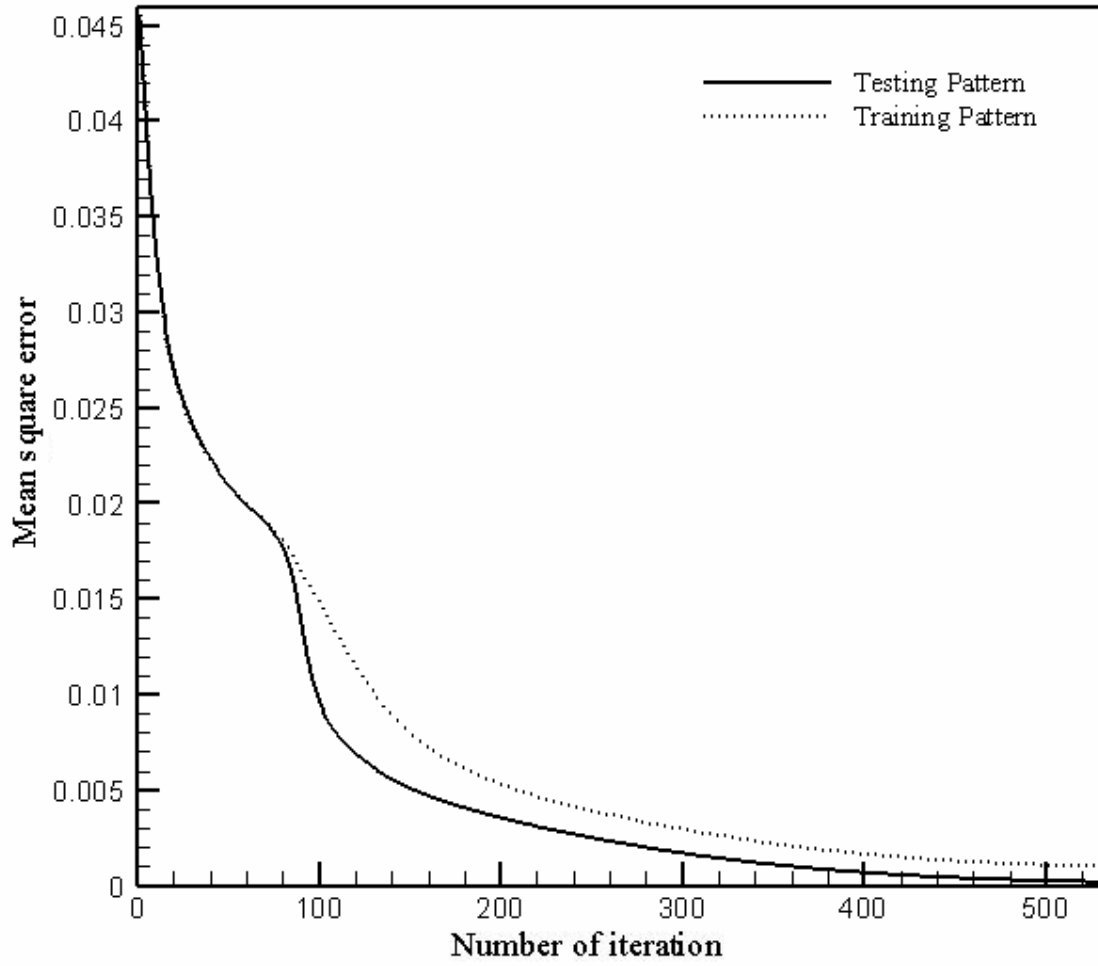


Fig. 12. Variation of mean square error with number of iteration for 6-5-1 neural network with $\alpha = 0.7$, $\eta = 0.8$ (considering chip thickness).

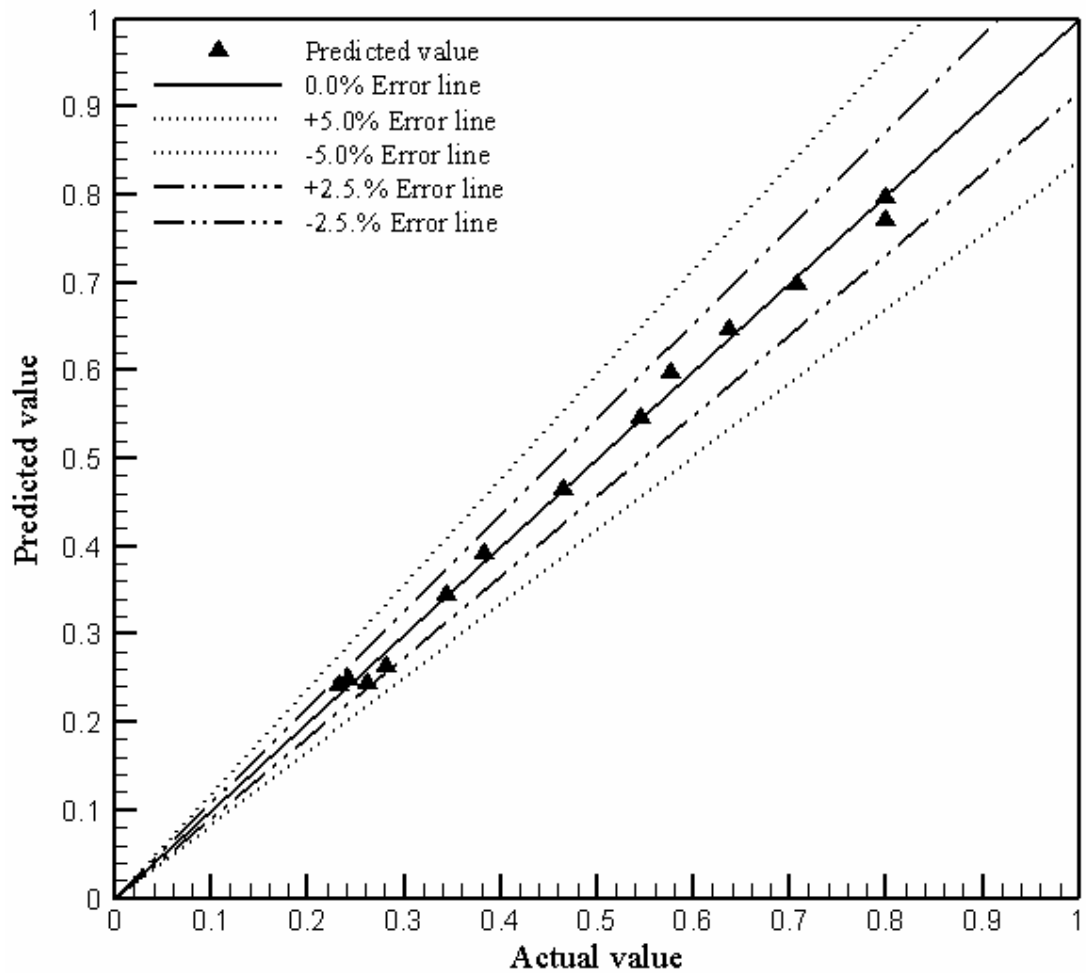


Fig. 13. Comparison between experimental value and predicted value of flank wear by 6-5-1 neural network (considering chip thickness).

Table 1
Experimental data for mild steel work-piece

<i>Serial no</i>	<i>Drill diameter (mm)</i>	<i>Speed (rpm)</i>	<i>Feed (mm/rev)</i>	<i>Force (N)</i>	<i>Torque (N-m)</i>	<i>Chip thickness (mm)</i>	<i>Wear (mm)</i>
1	10	500	0.13	3256	60.00	0.72	0.1
2	7.5	500	0.13	667	14.34	0.67	0.13
3	5	500	0.13	567	9.58	0.52	0.08
4	10	500	0.18	3298	62.51	0.82	0.17
5	7.5	500	0.18	692	14.58	0.76	0.14
6	5	500	0.18	584	10.12	0.41	0.04
7	10	500	0.25	3789	67.54	0.82	0.1
8	7.5	500	0.25	1004	17.22	0.77	0.3
9	5	500	0.25	956	14.56	0.53	0.15
10	10	400	0.13	3892	62.76	0.89	0.12
11	7.5	400	0.13	712	15.24	0.81	0.09
12	5	400	0.13	612	9.89	0.54	0.07
13	10	400	0.18	3935	64.72	1.1	0.07
14	7.5	400	0.18	744	15.65	0.94	0.13
15	5	400	0.18	624	10.96	0.55	0.03
16	10	400	0.25	4056	68.21	1.2	0.09
17	7.5	400	0.25	1045	17.3	0.95	0.08
18	5	400	0.25	997	15.32	0.72	0.14
19	10	630	0.13	2854	51.65	0.66	0.04
20	7.5	630	0.13	621	11.25	0.63	0.17
21	5	630	0.13	554	7.64	0.47	0.05
22	10	630	0.18	2988	57.62	0.77	0.11
23	7.5	630	0.18	675	12.15	0.69	0.07
24	5	630	0.18	569	8.22	0.49	0.04
25	10	630	0.25	3426	61.11	0.8	0.1
26	7.5	630	0.25	978	16.54	0.73	0.2
27	5	630	0.25	944	13.24	0.51	0.05
28	10	800	0.36	2547	48.95	0.87	0.0775
29	7.5	800	0.36	649	10.62	0.68	0.0525
30	5	800	0.36	523	6.24	0.48	0.045
31	10	800	0.5	3021	52.24	0.94	0.082
32	7.5	800	0.5	696	13.35	0.78	0.074
33	5	800	0.5	547	8.64	0.57	0.0675
34	10	800	0.71	3501	57.61	1.1	0.094
35	7.5	800	0.71	956	15.24	0.82	0.088
36	5	800	0.71	912	10.37	0.59	0.074
37	10	315	0.36	4114	71.56	1.15	0.096
38	7.5	315	0.36	1068	18.27	0.88	0.0832
39	5	315	0.36	1034	11.54	0.61	0.0725
40	10	315	0.5	4181	72.62	1.2	0.102
41	7.5	315	0.5	1112	19.44	0.84	0.085
42	5	315	0.5	1084	12.85	0.58	0.076
43	7.5	315	0.71	1434	23.62	0.88	0.105
44	5	315	0.71	1325	18.14	0.65	0.086
45	10	1000	0.36	2423	44.51	0.85	0.068
46	7.5	1000	0.36	584	6.47	0.72	0.044
47	5	1000	0.36	489	2.36	0.57	0.038
48	10	1000	0.5	2473	46.32	1.01	0.074
49	7.5	1000	0.5	607	7.38	0.95	0.062
50	5	1000	0.5	503	3.15	0.65	0.0575
51	7.5	1000	0.71	921	8.12	0.96	0.078
52	5	1000	0.71	884	4.57	0.66	0.065

Table 2

Training error for different neural network architectures (without considering chip thickness)

<i>Serial number</i>	<i>Neural network architecture</i>	<i>Momentum coefficient(α)</i>	<i>Learning rate(η)</i>	<i>Mean square error</i>	<i>Number of iteration</i>	<i>Maximum predicted error (%)</i>	<i>Minimum predicted error (%)</i>
1	5-3-1	0.7	0.8	0.00766	5076	55.1	2.02
2	5-3-1	0.8	0.9	0.00650	5394	61.0	3.71
3	5-3-1	0.5	0.6	0.00770	11002	51.1	1.1
4	5-3-1	0.6	0.4	0.00770	11340	42.3	0.4
5	5-3-1	0.3	0.3	0.00700	33371	33.5	0.56
6	5-4-1	0.7	0.8	0.0050	8214	95.1	3.2
7	5-4-1	0.8	0.9	0.0070	5048	54.2	1.2
8	5-4-1	0.5	0.6	0.0050	3737	81.4	3.4
9	5-4-1	0.6	0.4	0.0050	3816	75.4	3.7
10	5-4-1	0.3	0.3	0.0050	1068	56.5	3.2
11	5-5-1	0.7	0.8	0.0090	2554	43.5	1.1
12	5-5-1	0.8	0.9	0.0090	6146	48.1	0.5
13	5-5-1	0.5	0.6	0.0060	727	72.5	3.4
14	5-5-1	0.6	0.4	0.0060	458	55.2	5.7
15	5-5-1	0.3	0.3	0.0060	629	43.1	2.1

Table 3
 Training error for different neural network architectures (considering chip thickness)

<i>Serial number</i>	<i>Neural network architecture</i>	<i>Momentum coefficient (α)</i>	<i>Learning rate (η)</i>	<i>Mean square error</i>	<i>Number of iteration</i>	<i>Maximum predicted error (%)</i>	<i>Minimum predicted error (%)</i>
1	6-3-1	0.7	0.8	0.0035	6533	28.68	0.97
2	6-3-1	0.8	0.9	0.0035	5425	28.57	5.29
3	6-3-1	0.5	0.6	0.0032	16244	28.41	2.37
4	6-3-1	0.6	0.4	0.00770	18143	28.49	3.78
5	6-3-1	0.3	0.3	0.0028	1307	19.22	1.85
6	6-4-1	0.7	0.8	0.0028	14283	28.04	6.22
7	6-4-1	0.8	0.9	0.0030	8049	28.17	7.57
8	6-4-1	0.5	0.6	0.0050	13856	24.38	1.32
9	6-4-1	0.6	0.4	0.0050	16456	24.44	1.17
10	6-4-1	0.3	0.3	0.0050	34911	24.81	0.450
11	6-5-1	0.7	0.8	0.0010	530	7.465	0.00016
12	6-5-1	0.8	0.9	0.0060	4460	28.52	1.87
13	6-5-1	0.5	0.6	0.0010	885	7.94	0.021
14	6-5-1	0.6	0.4	0.0010	998	7.88	0.035
15	6-5-1	0.3	0.3	0.0060	1983	8.22	0.61